Consideration on appearance and disappearance of energy in superconductors during change in external magnetic field

Consideration on Appeared of Disappeared Energy in Superconductors during Changing External Magnetic Field

Teruo Matsushita, and Masaru Kiuchi

Department of Computer Science and Electronics, Kyushu Institute of Technology, Iizuka, Fukuoka 820-8502, Japan

*E-mail: matsushita.teruo391@mail.kyutech.jp

When flux lines are displaced in a superconductor by increasing the external magnetic field, the energy penetrating the superconductor is larger than the increase in the magnetic energy. In some case the energy coming out of the superconductor is larger than the decrease in the magnetic energy when the magnetic field is decreased, indicating an appearance of energy. These differences between the penetrating energy and change in the magnetic energy can be explained as a work done by the driving force against the pinning force that determines the magnetic flux distribution in the superconductor. The disappeared energy is dissipated or absorbed as an increase in the pinning energy. This indicates that the Maxwell theory is comprehensive also for electromagnetic phenomena in superconductors. The displacement of flux lines is also examined for the force-free state that is established in a current-carrying superconductor in a parallel magnetic field. Similar difference in the energy suggests existence of generalized driving force, i.e., a driving torque, since the Lorentz force is zero in this state. This clearly shows that the flux cutting event cannot be realized, since it is based on the magnetic interaction and the penetrated energy cannot be absorbed.

1. Introduction

Electromagnetic phenomena in superconductors such as non-dissipative current or energy loss are deeply associated with the energetic pinning interaction between quantized flux lines and defects called pinning centers. The center of each flux line is a singular point on which the gradient of the phase of the order parameter diverges, and the order parameter must be zero to avoid the divergence of the superconducting current density.[1)] As a result the central area of the flux line of a radius about the coherence length, ξ, is in the normal state. This area is called normal core. According to the Ginzburg-Landau theory, the energy density in the normal core is higher by the condensation energy density, ${B_c}^2/2\mu_0$, than in the surrounding superconducting region, where B_c is the thermodynamic critical field. When the normal core meets a normal precipitate, the length of the normal core that destroys the superconductivity becomes shorter, resulting in a state with a lower energy. Thus, normal precipitates work as attractive pinning centers.[2)]

When an electric current of density $\boldsymbol{J}$ is applied to a superconductor in a magnetic flux density $\boldsymbol{B}$, the Lorentz force $\boldsymbol{J} \times \boldsymbol{B}$ works on pinned flux lines in a unit volume. If the Lorentz force is stronger than the pinning force, the flux lines are driven into a flow state and an electromotive force is generated. The induced electric field is given by[3)]

$$\boldsymbol{E} = \boldsymbol{B} \times \boldsymbol{v}, \tag{1}$$

where $\boldsymbol{v}$ is the velocity of flux lines. Normal electrons inside the normal core are driven by the induced electric field, resulting in energy dissipation. Various irreversible phenomena in the superconductor caused by movement of flux lines are well described by the critical state model.[4)] The nature of these irreversible phenomena is non-ohmic, and the dissipated power is proportional to the electric field E and is called iron loss, while the dissipated power in common metals is proportional to E^2 and is called copper loss. The loss energies associated with magnetic hysteresis in ferromagnetic materials and friction belong to the former type.

This seems to be contradictory, since the original local phenomena associated with the energetic interaction with pinning centers are reversible. The irreversibility comes from unstable motion of flux lines driven from one pinning center to another by a Lorentz force[5)]. If we confine to the case of small displacement of flux lines inside a pinning potential, however, reversible flux motion can be observed.[6)]

When the magnetic field applied to the superconductor is changed, the internal magnetic flux distribution changes. The energy that comes in or goes out of the superconductor can be calculated using Poynting's vector. We treat various cases in this paper. For simplicity, it is

assumed that the critical current density, J_c, is constant within the superconductor during changing the external magnetic field based on Bean's model.[4)]

2. Transverse Field Geometry

The magnetic field produced by a current is perpendicular to the current. This field geometry is called transverse field. We assume for simplicity a wide superconducting slab that occupies $0 \le x \le 2d$ and apply an external magnetic field along the z-axis. From symmetry we have to consider only the half, $0 \le x \le d$. In the following we assume two cases; one is the case where the irreversible critical state model holds and the other is the case where the reversible phenomenon occurs.

2.1 Irreversible case

When the external field is increased from 0 to H_0, the critical state model describes that the internal magnetic flux distribution is given by

$$\begin{aligned} B_z(x) &= \mu_0(H_0 - J_c x); && 0 \le x \le H_0/J_c, \\ &= 0, && H_0/J_c < x \le d, \end{aligned} \tag{2}$$

where the above equation holds for $H_0 < J_c d$ (see Fig. 1). The current flows with the density J_c along the positive y-axis direction. When H_0 exceeds $J_c d$, the upper equation of Eq. (2) holds in the entire region ($0 \le x \le d$).

In this process the induced electric field is given by

$$E_y(x) = -\int_{H_0/J_c}^{x} \frac{\partial B_z(x)}{\partial t}\mathrm{d}x = \mu_0 \frac{\partial H_0}{\partial t}\left(\frac{H_0}{J_c} - x\right) \tag{3}$$

for $0 \le x < H_0/J_c$ and $E_y(x) = 0$ for $H_0/J_c < x \le d$. Hence, Poynting's vector ($\boldsymbol{S}_P = \boldsymbol{E} \times \boldsymbol{H}$) on the surface ($x = 0$) is

$$S_p = \frac{\mu_0}{J_c} {H_0}^2 \frac{\partial H_0}{\partial t} \tag{4}$$

and directed along the interior of the superconductor (the positive x-axis). Thus, the energy penetrating a unit surface area of the superconductor during increasing the external magnetic field from 0 to H_e is calculated as

$$U = \frac{\mu_0}{J_c}\int_0^{H_e} {H_0}^2 \mathrm{d}H_0 = \frac{\mu_0}{3J_c} {H_e}^3. \tag{5}$$

On the other hand, the total magnetic energy at the final state is

$$U_{\mathrm{m}} = \int_0^{H_{\mathrm{e}}/J_{\mathrm{c}}} \frac{\mu_0}{2}(H_{\mathrm{e}} - J_{\mathrm{c}}x)^2 \mathrm{d}x = \frac{\mu_0}{6J_{\mathrm{c}}} {H_{\mathrm{e}}}^3, \tag{6}$$

which is smaller than the input energy. Thus, some energy disappeared in the above process.

If we remember that Poynting's energy contains the term $\int \boldsymbol{E} \cdot \boldsymbol{J} \mathrm{d}t$ in addition to the magnetic energy, it is easy to find the reason for the above apparent discrepancy. In the present irreversible case the disappeared energy is speculated to be dissipated:

$$W = \int \mathrm{d}t \int_0^{H_0/J_{\mathrm{c}}} E_y(x) J_{\mathrm{c}} \, \mathrm{d}x = \frac{\mu_0}{2J_{\mathrm{c}}} \int_0^{H_{\mathrm{e}}} {H_0}^2 \mathrm{d}H_0 = \frac{\mu_0}{6J_{\mathrm{c}}} {H_{\mathrm{e}}}^3. \tag{7}$$

In fact, the following condition holds:

$$U = U_{\mathrm{m}} + W. \tag{8}$$

In this case the disappearance of energy is reasonable.

2.2 Reversible case

The electromagnetic phenomena are different from the above in reversible cases. The reversible state appears for example when the external magnetic field is slightly reduced after increasing to a sufficiently high value, H_{m}, as shown in Fig. 2. The initial magnetic flux distribution is given by

$$B_z(x) = \mu_0(H_{\mathrm{m}} - J_{\mathrm{c}}x). \tag{9}$$

When the external magnetic field is decreased by ΔH_{e}, the magnetic field distribution changes as

$$\begin{aligned} B_z(x) &= \mu_0(H_{\mathrm{m}} - J_{\mathrm{c}}x) - \Delta B(x); \\ \Delta B(x) &= \mu_0 \Delta H_{\mathrm{e}} \exp\left(-\frac{x}{{\lambda_0}'}\right), \end{aligned} \tag{10}$$

where ${\lambda_0}'$ is a characteristic length called Campbell's AC penetration depth. This is the pinning correlation length and is given by

$$\lambda_0' = \left(\frac{\mu_0 {H_{\mathrm{m}}}^2}{\alpha_{\mathrm{L}}}\right)^{1/2}, \tag{11}$$

where α_{L} is the Labusch parameter.[7] The change in the current density on the surface is given by $\Delta J = |{\mu_0}^{-1}(\partial \Delta B(x)/\partial x)_{x=0}| = \Delta H_{\mathrm{e}}/{\lambda_0}'$ and the reversible phenomenon continues in the whole superconductor until ΔJ increases to $2J_{\mathrm{c}}$. A further decrease in the external field leads to the penetration of the opposite critical state from the surface. In the AC measurement method the amplitude of AC magnetic flux Φ penetrating the superconducting slab is measured as a function of AC field amplitude h_0.[7] Then, the

penetration depth of the AC magnetic flux is determined with

$$\lambda' = \frac{1}{2\mu_0 w} \cdot \frac{\partial \Phi}{\partial h_0}, \tag{12}$$

where w is the width of the superconducting slab. In the case of irreversible penetration as described by the critical state model, simply we have

$$\Phi = \frac{\mu_0 w}{2J_c} {h_0}^2 \tag{13}$$

and Eq. (12) leads to $\lambda' = h_0/J_c$, as the critical state model predicts. On the other hand, in the reversible case where Eq. (10) holds we have

$$\Phi = w \int_0^d 2\mu_0 \, h_0 \exp\left(-\frac{x}{\lambda_0'}\right) \cong 2\mu_0 w h_0 \lambda_0', \tag{14}$$

where we assumed that d is much larger than λ_0' and ΔH_e corresponds to the peak to peak value, $2h_0$. Then, Eq. (12) leads to

$$\lambda' = \lambda_0'. \tag{15}$$

Figure 3 shows the experimental result of the field profile obtained with the AC measurement method:[8] When h_0 is sufficiently large, the field profile obeys the critical state model, while λ' approaches to a constant value λ_0' in the limit of small h_0.

When the external magnetic field is slightly decreased by Δh_e after increasing to H_m, the internal magnetic field distribution changes as

$$B_z(x) = \mu_0 \left[H_m - J_c x - \Delta h_e \exp\left(-\frac{x}{\lambda_0'}\right)\right]. \tag{16}$$

The electric field induced by decreasing the external field is

$$E_y(x) = \int_d^x \mu_0 \frac{\partial \Delta h_e}{\partial t} \exp\left(-\frac{x}{\lambda_0'}\right) dx \cong -\mu_0 \lambda_0' \frac{\partial \Delta h_e}{\partial t} \exp\left(-\frac{x}{\lambda_0'}\right), \tag{17}$$

where we assumed again that d is sufficiently longer than λ_0'. Hence, the energy that penetrates the superconductor during decreasing the external magnetic field by ΔH_e is

$$\begin{aligned} \Delta U = \int E_y(0)(H_m - \Delta h_e) dt &= -\mu_0 \lambda_0' \int_0^{\Delta H_e} (H_m - \Delta h_e) dh_e \\ &= -\mu_0 \lambda_0' \Delta H_e \left(H_m - \frac{\Delta H_e}{2}\right). \end{aligned} \tag{18}$$

On the other hand, the increase in the inner magnetic energy is

$$\begin{aligned} \Delta U_m &= -\frac{\mu_0}{2} \int_0^d \left\{(H_m - J_c x)^2 - \left[H_m - J_c x - \Delta H_e \exp\left(-\frac{x}{\lambda_0'}\right)\right]^2\right\} dx \\ &\cong -\mu_0 \lambda_0' \Delta H_e \left(H_m - J_c \lambda_0' - \frac{\Delta H_e}{4}\right). \end{aligned} \tag{19}$$

Then, we have

$$\Delta U - \Delta U_{\mathrm{m}} = -\mu_0 \lambda_0' \Delta H_{\mathrm{e}} \left(J_{\mathrm{c}} \lambda_0' - \frac{\Delta H_{\mathrm{e}}}{4} \right). \tag{20}$$

Hence, the energy that goes out of the superconductor during the process is larger than the decrease in the magnetic energy. Where does the energy of difference come from? Now we calculate the electric power. From Eq. (16) the current density is

$$J_y = -\frac{1}{\mu_0} \cdot \frac{\partial B_z}{\partial x} = J_{\mathrm{c}} - \frac{\Delta h_{\mathrm{e}}}{\lambda_0'} \exp\left(-\frac{x}{\lambda_0'} \right), \tag{21}$$

and the electric field is given by Eq. (17). Thus, the energy associated with the corresponding electric power is

$$\begin{aligned} W = \int \mathrm{d}t \int_0^d E_y J_y \, \mathrm{d}x &= -\int_0^{\Delta H_{\mathrm{e}}} \mathrm{d}\Delta h_{\mathrm{e}} \int_0^d \mu_0 \left[J_{\mathrm{c}} \lambda_0' \exp\left(-\frac{x}{\lambda_0'} \right) - \Delta h_{\mathrm{e}} \exp\left(-\frac{2x}{\lambda_0'} \right) \right] \mathrm{d}x \\ &= -\mu_0 \lambda_0' \Delta H_{\mathrm{e}} \left(J_{\mathrm{c}} \lambda_0' - \frac{\Delta H_{\mathrm{e}}}{4} \right). \end{aligned} \tag{22}$$

This is equal to $\Delta U - \Delta U_{\mathrm{m}}$ in Eq. (20). However, this energy is not dissipated, since it is negative. When the external magnetic field is increased from $H_{\mathrm{m}} - \Delta H_{\mathrm{e}}$ to H_{m}, the magnetic flux distribution is reversible following Eq. (16) and the energy of the same amount disappears.

The energy W in the above two cases is generally rewritten as

$$W = \boldsymbol{E} \cdot \boldsymbol{J} = (\boldsymbol{J} \times \boldsymbol{B}) \cdot \boldsymbol{v}, \tag{23}$$

where Josephson's relationship (1) is used for the electric field. Thus, the associated electric power is the rate of the work done by the Lorentz force. In fact, this was proved for the case of virtual displacement of flux lines by introducing strains to flux lines such as a gradient of the density[9] or bending,[10] which causes the magnetic pressure or line tension, respectively. The structures of magnetic flux lines that cause the Lorentz force are shown in Fig. 4.

In the first example the work done by the Lorentz force is dissipated as the pinning loss. In the second example, however, the work done by the Lorentz force is negative. It means that this energy was stored somewhere and appeared again in the decreasing field process. It is necessary to go back to the principle that determines the assumed magnetic flux distribution. All such distributions are realized by the flux pinning interaction. The critical state model describes the force-balance equation as

$$\boldsymbol{J} \times \boldsymbol{B} + \boldsymbol{F}_{\mathrm{p}} = 0, \tag{24}$$

where $\boldsymbol{F}_{\mathrm{p}}$ is the pinning force density. It is assumed as

$$\boldsymbol{F}_{\mathrm{p}} = -F_{\mathrm{p}} \boldsymbol{\delta}, \tag{25}$$

where F_{p} is an absolute value of $\boldsymbol{F}_{\mathrm{p}}$ and $\boldsymbol{\delta}$ is a unit vector directed along the Lorentz

force. This assumption that the pinning force always works opposite to the driving force is the origin of the irreversibility and is proved theoretically.[9, 11] The pinning loss in the first example is given by

$$W = -\boldsymbol{F}_{\mathrm{p}} \cdot \boldsymbol{v}. \tag{26}$$

The magnetic flux distribution in the second example is also derived from Eq. (24) that describes the force balance condition. The pinning force density in this case is, however, reversible with respect to the flux motion and its strength is below the critical value, $J_{\mathrm{c}}B$. The energetic situation is schematically illustrated in Fig. 5. The equilibrium position is determined by the condition:

$$\frac{\partial \mathcal{G}}{\partial \boldsymbol{u}} = 0, \tag{27}$$

where $\mathcal{G}$ is the Gibbs free energy given by

$$\mathcal{G} = U_{\mathrm{m}} + U_{\mathrm{p}} - (\boldsymbol{J} \times \boldsymbol{B}) \cdot \boldsymbol{u} \tag{28}$$

with U_{p} and $\boldsymbol{u}$ denoting the pinning energy and displacement of flux lines, respectively. Equation (27) describes the phenomena in the reversible state. From the relationship of

$$\frac{\partial U_{\mathrm{p}}}{\partial \boldsymbol{u}} = -\boldsymbol{F}_{\mathrm{p}}, \tag{29}$$

Eq. (24) is obtained in the critical state.[9] Hence, the energy introduced by the Lorentz force can be absorbed as an increase in the pinning energy. This is exactly shown in Appendix. The appeared energy in the second case was stored in the pinning energy during the former process of increasing field to H_{m}.

The reason why the energy is dissipated in the first case is that the pinning energy is full in the critical state, and hence, there is no room to store the energy additionally. As a result, all input energy is dissipated through unstable motion of depinned flux lines.[5] This situation can be explained using the force-displacement profile in Fig. 6(a). The starting point is the former critical state when the field was increased to H_{m}. Then, the flux lines are displaced to the opposite direction and the force-displacement relationship is linear with the slope of the Labusch parameter, α_{L}. When the displacement reaches twice the interaction distance, d_{i}, the opposite critical state is reached and the pinning force density is saturated for further displacement of flux lines. In this state, while new flux lines come in the pinning potential, some flux lines in the potential go out and the energy is dissipated. Thus, the Maxwell theory generally explains the origins of “dissipated energy” and “stored energy”.

3. Longitudinal Field Geometry

When a current is applied to a wide superconducting slab in a parallel magnetic field as schematically shown in Fig. 7, peculiar phenomena called longitudinal field effect occur. Those include dramatic increase in the critical current density,[12] break of the induced electric field from Eq. (1)[13] and observation of a negative potential drop along the length of the superconductor in the resistive state,[14, 15] etc. It is empirically known that the force-free state holds where the magnetic flux and current are locally parallel to each other:[16]

$$\boldsymbol{J} \times \boldsymbol{B} = 0. \tag{30}$$

The structure of flux lines in this state is schematically shown in Fig. 8.[17] The magnetic flux distribution below the critical state is given by

$$\boldsymbol{B} = (0, -B_0 \sin\theta(x), B_0 \cos\theta(x)) \tag{31}$$

with

$$\begin{aligned} \theta(x) &= \theta_0 - \alpha_{\mathrm{f}} x; && 0 \le x \le x_0 = \theta_0/\alpha_{\mathrm{f}}, \\ &= 0; && x > x_0, \end{aligned} \tag{32}$$

where θ_0 is the field angle on the surface ($x = 0$) and α_{f} represents the rotational shearing deformation that is related to the force-free critical current density $J_{\mathrm{c}\parallel}$ through

$$\alpha_{\mathrm{f}} = \frac{\mu_0 J_{\mathrm{c}\parallel}}{B_0}. \tag{33}$$

It is easy to show that the current density is

$$\boldsymbol{J} = \frac{1}{\mu_0} \mathrm{rot}\boldsymbol{B} = \left(0, -J_{\mathrm{c}\parallel} \sin\theta(x), J_{\mathrm{c}\parallel} \cos\theta(x)\right). \tag{34}$$

The magnetic flux distribution in the region $d \le x \le 2d$ is asymmetric with Eq. (31) with respect to the center, $x = d$, of the slab. The magnetic flux distribution in the force-free state was investigated by superposing a transverse (along the y-direction in the present geometry) magnetic field that induced the force-free current along the z-axis.[18] In this case the longitudinal component of the magnetic flux density is expected to be uniform inside the superconducting slab due to the abnormal transverse field effect.[19] Figure 9 shows the obtained distribution of transverse magnetic flux inside a superconducting slab when a small transverse in-plane magnetic field of amplitude h_0 was superposed to a large longitudinal magnetic field.[18] Since the superposed transverse magnetic field is sufficiently smaller than the longitudinal magnetic field, the result of Fig. 9 shows that the variation in the magnetic field angle is linear as expected in Eq. (32). Thus, the force-free state is realized under the longitudinal magnetic field geometry.

On the other hand, when there is no current, the structure of flux lines is uniform as in

Fig. 10. This suggests that the general driving force to release the deformed structure of flux lines is a torque to rotate the flux lines but not the force. In fact, the Lorentz force in this field configuration is zero as shown in Eq. (30).

To simply realize the force-free structure of flux lines it is enough to rotate the external magnetic field in a plane parallel to the surface of superconducting slab. In this case the magnetic flux distribution is symmetric with respect to the center, $x = d$, and a half of the magnetic flux distribution is the same as that in the case of applied transport current. In experiments a wide superconducting disk is rotated in a parallel magnetic field for simplicity,[20] which is relatively equivalent to a stationary superconducting disk in a rotating field. Since the rotation of magnetic flux is realized in the usual experimental procedure in which a parallel magnetic field is applied to a superconductor and then the transport current is applied,[21] the rotation motion of flux lines is essential. When the deformation in the force-free state is virtually introduced by rotating the external magnetic field, the input energy can be similarly estimated using Poynting's vector.[22] A brief derivation of the input energy is shown here. First we assume a uniform magnetic field B_0 along the z-axis inside the superconductor and rotate the magnetic field at the surface by angle θ_0 in the y-z plane to achieve the magnetic structure given by Eqs. (31) and (32) with keeping y_0 constant. The induced electric field is

$$\boldsymbol{E} = \left(0,\ E_y,\ E_z\right) \tag{35}$$

with

$$\begin{aligned} E_y(x) &= -\frac{B_0}{{\alpha_\mathrm{f}}^2}\cdot\frac{\partial\alpha_\mathrm{f}}{\partial t}[\sin\theta(x) - \theta(x)\cos\theta(x)], \\ E_z(x) &= \frac{B_0}{{\alpha_\mathrm{f}}^2}\cdot\frac{\partial\alpha_\mathrm{f}}{\partial t}\ [\theta(x)\sin\theta(x) - \cos\theta(x) + 1]. \end{aligned} \tag{36}$$

Hence, Poynting's vector on the surface is

$$S_\mathrm{P} = \frac{B_0^2}{\mu_0{\alpha_\mathrm{f}}^2}\cdot\frac{\partial\alpha_\mathrm{f}}{\partial t}(\theta_0 - \sin\theta_0). \tag{37}$$

The energy density that flows into the superconductor during increasing the angle from 0 to θ_m is

$$w = \frac{B_0^2}{\mu_0}\int_0^{\theta_\mathrm{m}}\frac{1}{\theta_0^2}(\theta_0 - \sin\theta_0)\mathrm{d}\theta_0 \cong \frac{B_0^2}{12\mu_0}\theta_\mathrm{m}^2. \tag{38}$$

This must be the work done by the driving torque, since the magnetic energy with density $B_0^2/2\mu_0$ does not change. The torque density is[22]

$$\Omega = \left|-\frac{\partial w}{\partial\theta_\mathrm{m}}\right| = \frac{B_0^2}{6\mu_0}\theta_\mathrm{m} = \frac{1}{6}B_0 J y_0. \tag{39}$$

The work done by the torque must be absorbed in the pinning energy to be compatible with the Maxwell theory. That is, the deformed structure of flux lines is stabilized by the pinning interaction. This explains the fact that the critical current density in the longitudinal magnetic field is also determined by the flux pinning strength.[12, 18, 23, 24] In usual experiments the transport current is applied to the superconductor after the longitudinal magnetic field is applied. In this case the strength of the magnetic field on the surface is also changed slightly, which causes the penetration of magnetic flux into the superconductor. The force-free structure is also established in this case. Hence, the above calculation is considered to hold valid generally.

4. Discussion

We have shown the apparent discrepancy of the difference between the penetrated energy and change in the magnetic energy for the cases of usual transverse magnetic field geometry and longitudinal one. In the former case the difference was shown to be the work done by the Lorentz force under the equilibrium condition given by Eq. (27). It shows that the Maxwell theory is in harmony with thermodynamics and comprehensively includes the reversible and irreversible flux pinning phenomena in superconductors as a part of magnetic phenomena, although superconductivity and flux pinning phenomena were not known in the 19th century when the Maxwell theory was completed.

A similar discrepancy appears when the force-free state is induced in the superconductor in a parallel magnetic field. This strongly indicates that the difference in the energy is also the work done by a generalized driving force, i.e., the force-free torque, and is absorbed as an increase in the pinning energy. This explains the experimental results that the critical current density is determined by the flux pinning strength in this field geometry also.[12, 18, 23, 24] Under the rotation motion of flux lines it can be shown that the induced electric field is almost parallel to the external magnetic field, which shows deviation from Josephson's relationship (1). Equation (36) shows actually the direction of the electric field on the surface; $E_y(0)/E_z(0)$ is approximately given by $-(2/9)\theta_0$ for small rotation angle θ_0. A similar result was obtained in the condition of experiments.[21, 25]

The solution of rotating flux motion was obtained from the continuity equation of flux lines:

$$\frac{\partial \boldsymbol{B}}{\partial t} = -\mathrm{rot}(\boldsymbol{B} \times \boldsymbol{v}). \tag{40}$$

Here we derive the velocity of flux lines in the above case. If we assume that $\boldsymbol{v}$ has a

single x component that depends only on x, it is easy to show that there is no solution. We assume as

$$\boldsymbol{v} = (0,\ v_y,\ v_z). \tag{41}$$

Under the variation in the magnetic flux distribution that corresponds to Eq. (36) for the electric field, we have

$$\begin{aligned} -B_0\sin\theta\frac{\partial v_z}{\partial z} - B_0\cos\theta\frac{\partial v_y}{\partial z} &= B_0\cos\theta\frac{\partial \theta}{\partial t}, \\ B_0\sin\theta\frac{\partial v_z}{\partial y} + B_0\cos\theta\frac{\partial v_y}{\partial y} &= B_0\sin\theta\frac{\partial \theta}{\partial t}. \end{aligned} \tag{42}$$

If we assume as

$$v_y = -r\cos\ \theta\frac{\partial \theta}{\partial t}, \qquad v_y = -r\sin\theta\frac{\partial \theta}{\partial t}, \tag{43}$$

and

$$r = (y - y_0)\sin\theta + (z - z_0)\cos\theta \tag{44}$$

with $(x,\ y_0,\ z_0)$ denoting the rotation center in the y-z plane, it is easy to find that Eqs. (43) and (44) satisfy Eq. (42). In Eq. (44) r gives the radius of rotation. It is evident that the electric field is not given by Eq. (1) but follows in the form:

$$\boldsymbol{E} = \boldsymbol{B} \times \boldsymbol{v} - \nabla\phi, \tag{45}$$

where ϕ is a scalar function. It should be noted that ϕ is not an electrostatic potential, since the electric field is induced by Faraday's law. Since the scalar product of the first term with the current density $\boldsymbol{J}$ is zero, the important component associated with the energy consumption is contained in the second term. A similar flux motion with a component along the x-axis was obtained for usual experimental condition.[21)]

On the other hand, the flux cutting model was proposed for explaining compatibility between the steady resistive state and constant longitudinal magnetization.[26)] Appearance of the resistance was attributed to continuous penetration of transverse field component based on Eq. (1), while the constant longitudinal magnetization indicated unchanged distribution of the longitudinal field component. Another flux cutting model, the direct flux cutting model, was proposed for explaining the experimental result that the AC electric field induced by a superposed small AC current was almost parallel to the longitudinal direction, showing a break of Josephson's relationship (1).[13)] It was assumed that only the transverse AC self-field penetrated the superconductor cutting each other with longitudinal DC field.

The assumption of the flux cutting can also be directly denied by the above discussion

on the energy penetration during the achievement of the force-free state. The input energy during the process must be absorbed as an increase in the pinning energy to satisfy the principle of energy conservation. This insists that the flux cutting must be replaced by another mechanism of interaction with the flux pinning. It is different from a simple magnetic interaction between flux lines with a tilted angle assumed in Ref. 27. In other words, the flux cutting, i.e., a kind of magnetic interaction cannot absorb the input energy, since the magnetic energy is unchanged. This scenario of energetic interaction indicates a reversible behavior of flux lines below some threshold. In fact the penetration depth of AC transverse field component approaches tens of micrometers in the limit of zero field amplitude in Fig. 9. Since the flux line spacing at this DC magnetic field (0.290 T) is about 90 nm, the variation in the magnetic flux distribution penetrates over hundreds of rows of flux lines. However, the processes of flux cutting such as direct flux cutting[13] and intersection and cross-joining[28, 29] seem to be incompatible with the reversible penetration of the transverse field component for such a long distance, since the irreversible flux cutting must be completed to start the interaction with flux lines on the next row.

On the other hand, the rotational flux motion driven by the torque explains the deviation from Josephson's relationship as discussed in the above. In the resistive state above the critical current density it is considered that a helical flux flow is initiated by the driving torque to satisfy the steady condition.[30] Note that a simple rotation itself does not satisfy the steady condition. This explains a helical electric field structure with a negative voltage region where the flux lines go out of the superconductor. Such a break of helical symmetry cannot be derived by the mechanism of uniform flux cutting. This theoretical prediction was confirmed by the experimental result showing that Poynting's vector is directed outward where the negative voltage appears.[15] The flux cutting event has also been assumed to explain other phenomena.[31] However, the problematic points in such assumption were argued in various aspects in Ref. 32.

The problem in the flux cutting model arises from the assumption of similarity between mechanical motion and flux motion based on Eq. (1). For this reason it was discussed[33] that flux lines must move translationally without rotation, since the rotational motion breaks the symmetry with larger loss at a longer distance from the rotation center. However, this equation does not hold and such a similarity is broken in the longitudinal field configuration. In fact, the solution of the continuity equation (40) shows compatibility between the rotation motion and symmetry. It is important to exactly understand the solution of such a fundamental equation without biased concept.

5. Conclusions

In this paper the energy flow during the displacement of flux lines in the superconductor was investigated using Poynting's vector. A part of energy appears or disappears depending on the process of displacement. This is the work done by the Lorentz force against the pinning force under the transverse magnetic field configuration. It is dissipated as Joule heat when the magnetic behavior obeys the irreversible critical state model. On the other hand, it is stored in or supplied from the pinning energy in the regime of reversible flux motion. This shows us the rigor of the Maxwell theory that includes the flux pinning as a kind of magnetic phenomena.

The same investigation was done for the magnetic phenomena in the current-carrying superconductor in the longitudinal magnetic field configuration. The energy penetrates into the superconductor during rotation of flux lines to introduce the force-free structure, while the magnetic energy does not change. The penetrated energy must be the work done by the driving torque against the pinning interaction that keeps the distorted force-free structure of flux lines. Thus, it can be concluded that this torque drives the flux lines instead of the Lorentz force. As a result, peculiar longitudinal field effects such as enhancement of the critical current density due to different efficiency of flux pinning, deviation of induced electric field from Eq. (1) and the electric field structure in the resistive state are comprehensively explained, and such a rotation motion of flux lines is supported by the solution of the continuity equation of flux lines.

Appendix

When the external magnetic field is slightly decreased by ΔH_{e} after increasing to H_{m}, the magnetic flux distribution is given by Eq. (10). If ΔH_{e} is sufficiently smaller than H_{m}, the continuity equation (40) leads to

$$H_{\mathrm{m}}\frac{\partial}{\partial x}u'(x) = -\Delta H_{\mathrm{e}}\exp\left(-\frac{x}{\lambda_0{}'}\right), \tag{A.1}$$

where $u'(x)$ is the displacement of flux lines from the initial critical state. This is obtained as

$$u'(x) = \frac{\Delta H_{\mathrm{e}}}{H_{\mathrm{m}}}\ \exp\left(-\frac{x}{\lambda_0{}'}\right). \tag{A.2}$$

All flux lines stay at the position of $u = 2d_i$ and the pinning energy density is $(1/2)\alpha_{\mathrm{L}}{d_{\mathrm{i}}}^2$ in the initial critical state (see Fig. 6(b)). Hence, the change in the pinning energy

in a unit surface area is

$$\frac{1}{2}\alpha_{\mathrm{L}}\int_0^d \left[\left(d_{\mathrm{i}}-u'(x)\right)^2-{d_{\mathrm{i}}}^2\right]\mathrm{d}x=-\mu_0\lambda_0'\Delta H_{\mathrm{e}}\left(J_{\mathrm{c}}\lambda_0'-\frac{\Delta H_{\mathrm{e}}}{4}\right), \qquad (\mathrm{A}.3)$$

where we have used Eq. (11). This is equal to the work done by the Lorentz force given by Eq. (22).

References

1) T. Matsushita: *Flux Pinning in Superconductors* (Springer, Berlin, 2014) 2nd ed., p. 15.

2) T. Matsushita: *Flux Pinning in Superconductors* (Springer, Berlin, 2014) 2nd ed., p. 214.

3) B. D. Josephson: Phys. Lett **16** (1965) 242.

4) C. P. Bean: Phys. Rev. Lett. **8** (1962) 250.

5) T. Matsushita: J. Phys. Soc. Jpn. **84** (2015) 034705.

6) T. Matsushita: *Flux Pinning in Superconductors* (Springer, Berlin, 2014) 2nd ed., p. 114

7) A. M. Campbell: J. Phys. C **2** (1969) 1492.

8) T. Matsushita, T. Honda and K. Yamafuji, Mem. Fac. Eng., Kyushu Univ. **43** (1983) 233 (see also T. Matsushita: *Flux Pinning in Superconductors* (Springer, Berlin, 2014) 2nd ed., p. 193).

9) T. Matsushita: Jpn. J. Appl. Phys. **51** (2012) 010109.

10) T. Matsushita: *Flux Pinning in Superconductors* (Springer, Berlin, 2014) 2nd ed., p. 407.

11) T. Matsushita: Physica C **243** (1995) 312.

12) G. W. Cullen and R. L. Novak: Appl. Phys. Lett. **4** (1964) 147.

13) J. R. Cave, J. E. Evetts and A. M. Campbell: J. Phys. (Paris) **39** (1978) C6-614.

14) T. Ezaki and F. Irie: J. Phys. Soc. Jpn. **40** (1976) 382.

15) T. Matsushita, A. Shimogawa and M. Asano: Physica C **298** (1988) 115.

16) C. J. Bergeron: Appl. Phys. Lett. **3** (1963) 63.

17) A. M. Campbell and J. E. Evetts: Adv. Phys. **21** (1972) 199, see p. 250.

18) A. Kikitsu, Y. Hasagawa and T. Matsushita: Jpn. J. Appl. Phys. **25** (1986) 32.

19) K. Funaki and K. Yamafuji: Jpn. J. Appl. Phys. **21** (1982) 299.

20) J. R. Cave and M. A. R. LeBlanc: J. Appl. Phys. **53** (1982) 1631 (See Fig. 1).

21) T. Matsushita, Y. Hasegawa and J. Miyake: J. Appl. Phys. **54** (1983) 5277.

22) T. Matsushita: J. Phys. Soc. Jpn. **54** (1985) 1954.

23) F. Irie, T. Matsushita, S. Otabe, T. Matsuno and K. Yamafuji,:Cryogenics **29** (1989) 317.

24) T. Matsushita, Y. Miyamoto, A. Kikitsu and K. Yamafuji: Jpn. J. Appl. Phys. **25** (1986) L725.

25) T. Matsushita: *Flux Pinning in Superconductors* (Springer, Berlin, 2014) 2nd ed., p. 157.

26) D. G. Walmsley: J. Phys. F **2** (1972) 510.

27) E. H. Brandt, J. R. Clem and D. G. Walmsley: J. Low Temp. Phys. **37** (1979) 43.

28) J. R. Clem: J. Low Temp. Phys. **38** (1980) 353.

29) E. H. Brandt: J. Low Temp. Phys. **39** (1980) 41.

30) T. Matsushita and F. Irie: J. Phys. Soc. Jpn. **54** (1985) 1066.

31) See for example, T. Matsushita: *Flux Pinning in Superconductors* (Springer, Berlin, 2014) 2nd ed., p. 144.

32) T. Matsushita: Jpn. J. Appl. Phys. **51** (2012) 010111.

33) A. M. Campbell and J. E. Evetts; Adv. Phys. **21** (1972) 199 (See p. 250).

Figure Captions

Fig. 1. Magnetic field distribution in the initial increasing field process.

Fig. 2. Magnetic field distribution in the case where the external magnetic field is slightly decreased after reaching a sufficiently high value, H_{m}. The broken line shows the prediction of the critical state model.

Fig. 3. Field profile obtained using the AC inductive method for Nb-50at%Ta at 0.336 T.[8] The penetration depth λ' in the abscissa is plotted as a function of the AC field amplitude $\mu_0 h_0$ in the ordinate.

Fig. 4. Distorted structures of magnetic flux lines that cause the Lorentz force: (a) gradient of magnetic flux density and (b) bending deformation. The restoring forces shown by the arrows are magnetic pressure and line tension, respectively.

Fig. 5. Gibbs free energy g vs. displacement of flux lines $u = |\boldsymbol{u}|$.

Fig. 6. (a) Force-displacement profile starting from the critical state to the opposite critical state and (b) the pinning energy density. The characteristics are reversible within the displacement by $2d_{\mathrm{i}}$. When the displacement exceeds $2d_{\mathrm{i}}$, the phenomenon becomes irreversible.

Fig. 7. Configuration of external magnetic field (H_{e}) and current (I) in which the longitudinal field effect is observed.

Fig. 8. Structure of distorted flux lines in the force-free state with the force-free current.

Fig. 9. Distribution of transverse magnetic field component in superconducting Nb-50at%Ta slab obtained using the AC inductive method at 0.290 T.[18]

Fig. 10. Structure of flux lines with no distortion.

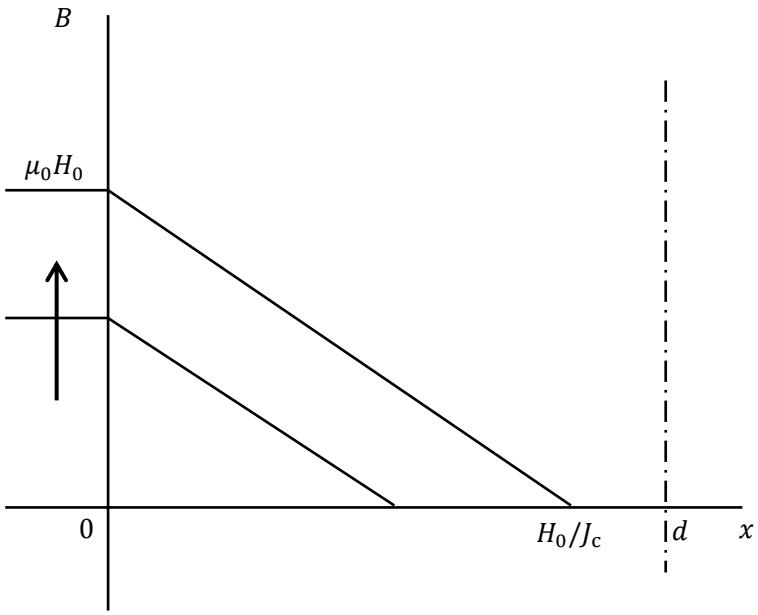

Fig.1. (black and white)

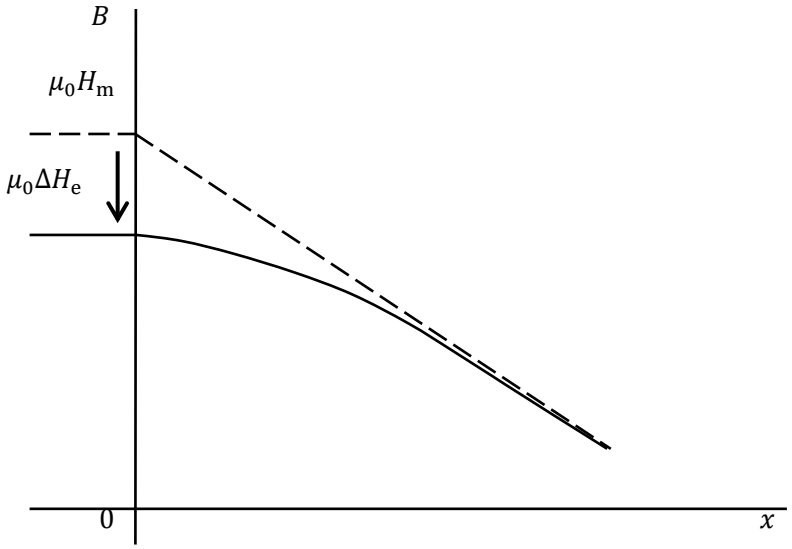

Fig. 2. (black and white)

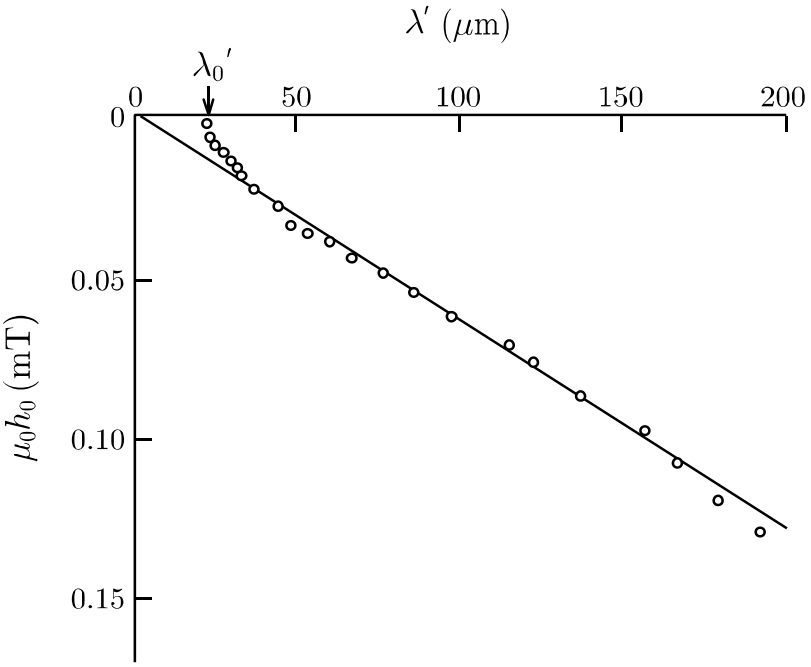

Fig. 3. (black and white)

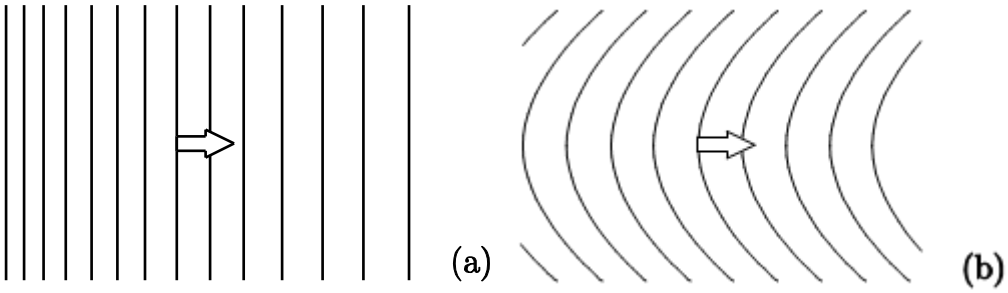

Fig. 4. (black and white)

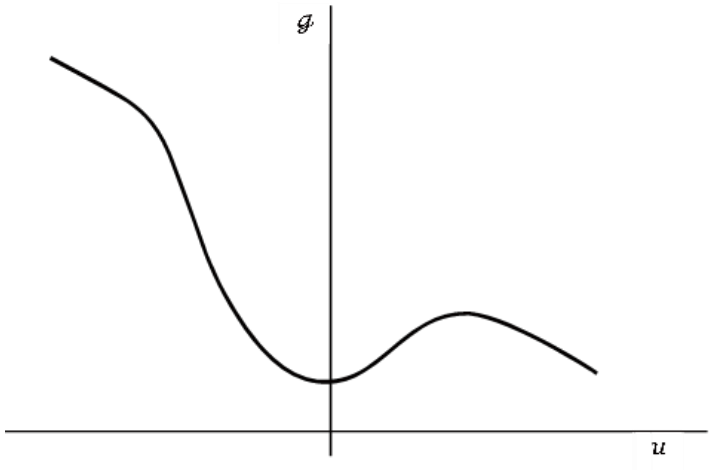

Fig. 5. (black and white)

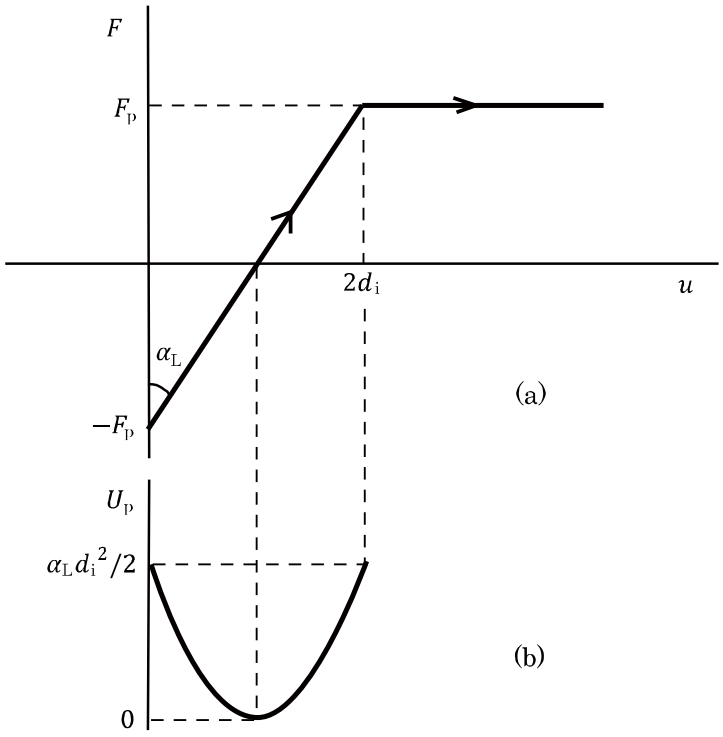

Fig. 6. (black and white)

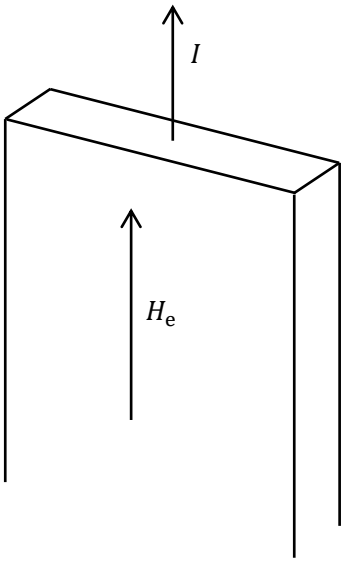

Fig. 7. (black and white)

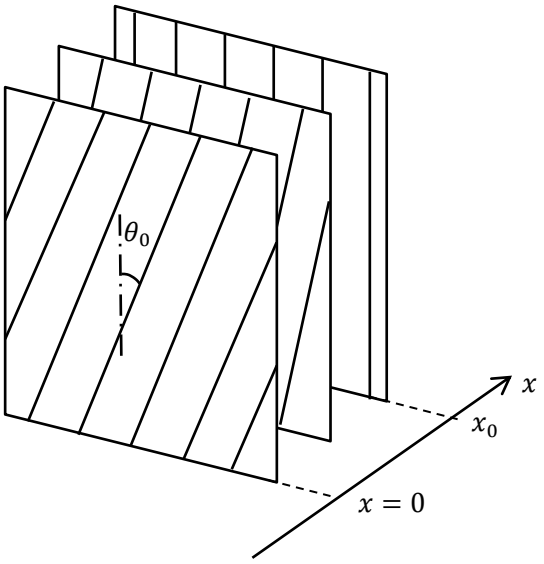

Fig. 8. (black and white)

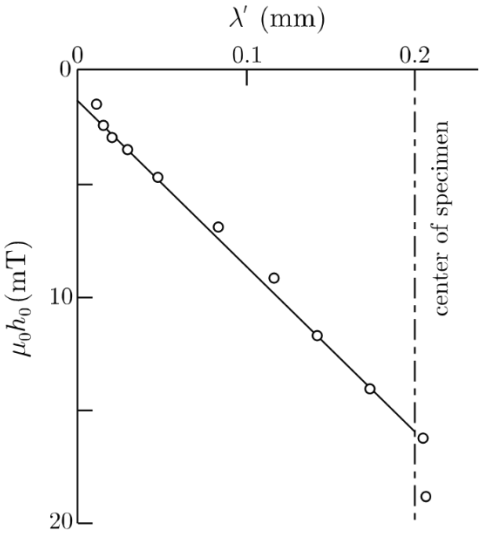

Fig. 9. (black and white)

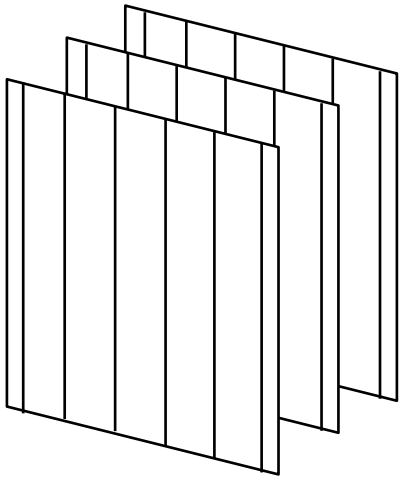

Fig. 10. (black and white)